

# The calculation of the campaign of reactor RITM-200

**D E Savitsky and A V Kuzmin**

The Butakov Research Center, Tomsk Polytechnic University, Tomsk, Russia

E-mail: [denis\\_savickii96@mail.ru](mailto:denis_savickii96@mail.ru)

**Abstract.** In this paper, the campaign of RITM-200 reactor was calculated. The duration of the campaign was determined taking the net capacity factor into consideration. The calculated duration concurred with the known data. The neutron parameters were calculated using the effective temperature method. The presence of burnable absorber rods was taken into account. Their effect was considered using the diffusional approach. The iterative computations were used to finally determine the temperature of the neutron gas. At the end, the reactivity curve displaying different effects inside fuel, namely fuel and gadolinium burn-out, the poisoning and slugging was drawn.

## 1. Introduction

RITM-200 is the newest reactor for the icebreaking fleet developed by JSC OKBM Afrikantov. Its appearance is presented in Figure 1. It is designed to produce 175 MWt (55 MWe) to power Project 22220 icebreakers, the first of which entered service in the May of 2019. The RITM-200 is an integrated PWR type, i.e. it contains the equipment of the first circuit inside the vessel of the reactor. One of the features of RITM-200 is the refuelling period, which is up to 7 years. In this paper, the calculation of the refuelling period was carried out using the effective temperature method.



**Figure 1.** View of RITM-200.

## 2. The core description

The core contains 199 fuel assemblies. According to [1] the structure of the fuel assembly remained the same as in KLT-40S reactor. Each assembly has 69 fuel rods, 9 burnable type-one absorber rods and 6 type-two absorber rods, and 7 control rods in the center of the fuel assembly (Figure 2). Burnable type-



Content from this work may be used under the terms of the [Creative Commons Attribution 3.0 licence](https://creativecommons.org/licenses/by/3.0/). Any further distribution of this work must maintain attribution to the author(s) and the title of the work, journal citation and DOI.

one and type-two absorber rods are distinguished by the density of burnable absorber [1]: in type-one rod gadolinium density equals  $2.7 \text{ g/cm}^3$ , whereas in type-two rod gadolinium density equals  $1.4 \text{ g/cm}^3$ .

As the structure of the fuel assembly of RITM-200 is the same with the structure of the fuel assembly of KLT-40S, the mean uranium enrichment can be inferred from the data in [1] of the mass of Uranium-235 and the whole uranium load in KLT-40S. Hence the average enrichment is 14.06%.

Structurally, the fuel rod is a smooth rod with a diameter of 6.8 mm with a length of the fuel containing part of 1200 mm. Chromium-nickel alloy 42HNM (41% Cr, 0.2% Mn, 0.2% Mo, 56.1% Ni, etc.) is used as fuel cladding, because it has a higher corrosion resistance and resistance to disruption of the water chemistry regime than the traditional zirconium alloy E110. The thickness of the cladding is 0.5 mm. Inside the cladding, there is a dispersed fuel composition consisting of uranium dioxide granules with low porosity and a silumin (87% Al, 11% Si, 2% Ni). The volume fraction of uranium-containing material in the fuel pellet is 66%.

A pure gadolinium oxide is not used as a burnable absorber. Instead of it a burnable absorber rods contain composition  $3\text{Gd}_2\text{O}_3 \cdot \text{Nb}_2\text{O}_5 \cdot \text{ZrO}_2$  which has less swelling as a result of neutrons absorbing.

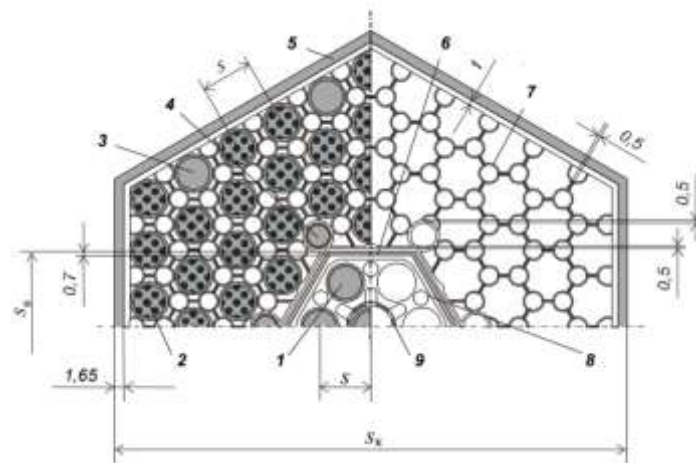


**Figure 2.** RITM-200 fuel assembly structure: 1 – control rod, 2 – fuel rod, 3 – burnable absorber type-one rod, 4 – burnable absorber type-two rod, 5 – casing, 6 – displacer, 7 – spacing grid, 8 – control rods spacing plates, 9 – central tube.

### 3. The effective temperature method

In calculations of neutron behavior, all cross sections should be related to the average neutron speed. It should be noted that the Maxwell thermal neutron spectrum gradually passes into the spectrum of slowing down neutrons at a temperature of 293 K at an energy that approximately equals 0.2 eV which is called the "sewing energy". The "sewing energy" is illustrated in Figure 3.

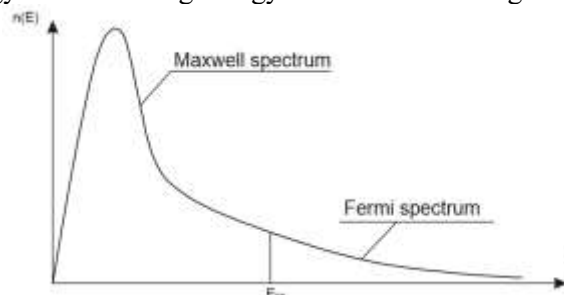


**Figure 3.** Illustration of the "sewing energy".

In reality, the thermal neutrons distribution does not exactly coincide with the Maxwell distribution, since the absorption of thermal neutrons takes place, the spectrum is shifted to higher energies.

For convenience of calculations in the theory of reactors, it is assumed that thermal neutrons are distributed over the Maxwell spectrum, but have a higher effective temperature (the temperature of the neutron gas —  $T_{ng}$ ), which exceeds the moderator temperature.

The gadolinium cross sections cannot be used for finding the temperature of the neutron gas directly, as due to its big cross-section of absorption ( $\sigma_a = 49000$  barns [2]) the strong degradation of the neutron flux occurs in the burnable absorber rod and only the part of the gadolinium volume participates in the neutron absorption. This part is described by the shielding coefficient  $k_s$ .

$$k_s = \frac{F_{ba}}{F_c} \quad (1)$$

Where  $F_{ba}$  is the thermal neutron flux in burnable absorber rods,  $F_c$  is the average thermal neutron flux in the core. As is it shown in the Figure 4, the thermal neutron flux in burnable absorber rods is lower than the average thermal neutron flux due to high absorption. The fall in the  $F_{ba}$  decreases throughout the campaign as the density of gadolinium declines.

Therefore, to find  $T_{ng}$  it is essential to know  $k_s$ .

$$T_{ng} = T_0 \left[ 1 + C \left( \frac{\sum_j (VN\sigma_a(0.025 \text{ eV}))_j}{\sum_j (VN\zeta\sigma_s(1 \text{ eV}))_j} \right) \cdot \sqrt{\frac{293.6}{T_0}} \right] \quad (2)$$

Where  $T_0$  is the moderator temperature,  $V$  and  $N$  are volumes per one fuel rod and densities of components of the core,  $\sigma_a(0.025 \text{ eV})_j$  and  $\sigma_s(1 \text{ eV})_j$  are thermal cross-sections of absorption and scattering, respectively, of materials of the core,  $C$  is the empirical constant which equals 1.70 for PWR type reactors.  $\zeta$  is a mean logarithmic loss of energy in a collision of a neutron and a nucleus.

The parameters of core components necessary to calculate  $T_{ng}$  by (2) are presented in table 1.

**Table 1.** Parameters of core components except burnable absorbers

Materials	$VN\sigma_a(0.025 \text{ eV})$ (cm)	$VN\zeta\sigma_s(1 \text{ eV})$ (cm)
U-235	0.310	$5.26 \cdot 10^{-5}$
U-238	$7.55 \cdot 10^{-3}$	$2.10 \cdot 10^{-4}$
O-16	$1.75 \cdot 10^{-6}$	$2.93 \cdot 10^{-3}$
H2O	0.0109	0.71
Al-27	$8.39 \cdot 10^{-4}$	$3.93 \cdot 10^{-4}$
Si-28	$7.09 \cdot 10^{-5}$	$6.78 \cdot 10^{-5}$
Zr-91	$6.75 \cdot 10^{-4}$	$5.00 \cdot 10^{-4}$
Cr-52	0.0128	$5.94 \cdot 10^{-4}$
Mo-96	$1.4 \cdot 10^{-4}$	$6.53 \cdot 10^{-6}$
Ni-59	0.0220	$2.88 \cdot 10^{-3}$
Mn-55	$2.53 \cdot 10^{-4}$	$1.43 \cdot 10^{-6}$

In RITM-200 the mean moderator temperature is  $296.5^\circ\text{C}$  ( $569.5 \text{ K}$ ).

#### 4. Burnable absorber rod calculation

To calculate the shielding coefficient, it is necessary to represent the core as a block with the burnable absorber rod in the center of the block and everything else around it, as it is drawn on the Figure 4.

Other elements except gadolinium may be dismissed as their yield is little.

The calculation is iterative, thus the initial approximation of the temperature of the neutron gas should be assumed. After the assumption the average cross-sections of absorption and fission in the Maxwell spectrum should be calculated.

- For  $1/v$  absorbers:

$$\bar{\sigma}_a = \sigma_{a0} \cdot 0.884 \sqrt{\frac{293}{T_{ng}}} \quad (3)$$

- For non-1/v absorbers:

$$\bar{\sigma}_a = \sigma_{a0} \cdot 0.884 \cdot G_a \sqrt{\frac{293}{T_{ng}}} \quad (4)$$

$$\bar{\sigma}_f = \sigma_{f0} \cdot 0.884 \cdot G_f \sqrt{\frac{293}{T_{ng}}} \quad (5)$$

Transport cross-section:

$$\bar{\sigma}_{tr} = \bar{\sigma}_a + \bar{\sigma}_s \cdot (1 - \mu) \quad (6)$$

Where  $\mu = \frac{2}{3A}$ ,  $A$  is the atomic number of the nuclide.

Where  $G_a$  and  $G_f$  are the thermal correction factors for non-1/v absorbers for absorption and fission cross-sections, respectively.

$$r_1 = \sqrt{4 \cdot V_{Gd} / \pi} \quad (7)$$

Then the average macroscopic cross-section of absorption ( $\Sigma_a$ ) and transport cross-section ( $\Sigma_{tr}$ ) are calculated in both zones: burnable absorber zone and multiplying zone. Index 2 refers to the multiplying zone.

$$\Sigma_a^{Gd} = \sum_i (VN\sigma_a)_{Gd} / V_{Gd} \quad (8)$$

$$\Sigma_{tr}^{Gd} = \sum_i (VN\sigma_{tr})_{Gd} / V_{Gd} \quad (9)$$

$$\Sigma_a^2 = \sum_i (VN\sigma_a)_2 / V_2 \quad (10)$$

$$\Sigma_{tr}^2 = \sum_i (VN\sigma_{tr})_2 / V_2 \quad (11)$$

Then the material parameters of the media are determined:

$$\chi_{Gd} = \sqrt{3\Sigma_a^{Gd}\Sigma_{tr}^{Gd}} \quad (12)$$

$$\chi_2 = \sqrt{3\Sigma_a^2\Sigma_{tr}^2} \quad (13)$$

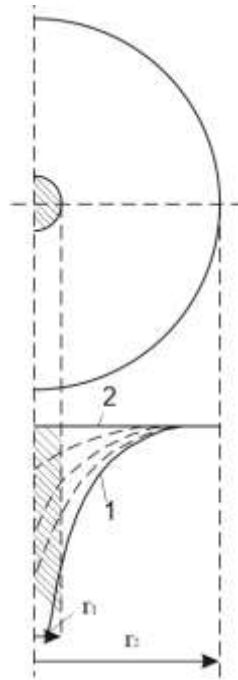


**Figure 4.** Thermal neutron flux density distribution near burnable absorber rod: 1 – In the beginning of the campaign with initial burnable absorber density; 2 – at the end of campaign when the burnable absorber is completely burned out,  $r_1$  – the radius of burnable absorber rod,  $r_2$  – the radius of volume of water per one burnable absorber rod.

Effective macroscopic cross-section of absorption of gadolinium:

$$\Sigma_{Gd}^{ef} = \frac{\Sigma_{Gd}}{1 + (3.593 \cdot \frac{r_1}{2} - \gamma_d) \cdot \Sigma_{Gd} + 0.426 \cdot (\frac{r_1}{2} \Sigma_{Gd})^2} \quad (14)$$

Where

$$\gamma_d = \frac{\chi_2 r_1}{2 \Sigma_a^2} \cdot \frac{K_0(\chi_2 r_1)}{K_1(\chi_2 r_1)} + \frac{1}{\Sigma_a^{Gd}} \left[ \frac{\chi_2 r}{2} \cdot \frac{I_0(\chi_{Gd} r_1)}{K_1(\chi_{Gd} r_1)} - 1 \right] \quad (15)$$

The shielding coefficient:

$$k_s = \frac{1}{1 + \gamma_d \Sigma_{Gd}^{ef}} \quad (16)$$

## 5. Computation of the effective multiplication factor

As the shielding coefficient is determined, the temperature of the neutron gas is to be calculated by (2), where the densities of absorber rod components ought to be multiplied by  $k_s$  to take into account the part of the rod that does not participate in the process of absorbing neutrons.

If calculated  $T_{ng}$  differs by more than 3 percent from the initial assumption, the calculation is repeated from the beginning using  $T_{ng}$  calculated in the previous iteration by (16). Equation (2) is omitted as  $T_{ng}$  is known from the previous iteration.

The iterative calculation is stopped when found temperature of the neutron gas by (16) concurs with one determined in the previous iteration.

As a result of the calculation,  $T_{ng} = 1050$  K.

The average cross-sections of fission for U-235:  $\bar{\sigma}_f = 258.91$  barn;  $\Sigma_f = 0.5516$  cm<sup>-1</sup>.

The average cross-sections of all core materials are presented in table 2.

The next step is the calculation of the effective multiplication factor  $k_{eff}$  by the six-factor formula [3]:

$$k_{eff} = \eta f p \varepsilon P_{FNL} P_{TNL}, \quad (17)$$

Where  $\eta$  is Thermal Fission Factor;  $f$  is the thermal utilization factor,  $p$  is the resonance escape probability,  $\varepsilon$  is the fast fission factor,  $P_{FNL}$  is the fast non-leakage probability, and  $P_{TNL}$  is the thermal non-leakage probability. Calculation formulae for each factor are given in [4].

**Table 2.** Average microscopic and macroscopic cross-sections of absorption of main core materials.

Materials	$VN\sigma_a(0.025 \text{ eV})$ (cm)	$VN\zeta\sigma_s(1 \text{ eV})$ (cm)
U-235	306.64	0.6822
U-238	1.33	0.1342
O-16	$1.3 \cdot 10^{-4}$	0.1092
H2O	0.33	0.8972
Al-27	0.11	0.0268
Si-28	0.08	0.0046
Zr-91	0.09	0.2661
Cr-52	1.52	0.1973
Mo-96	1.30	0.0035
Ni-59	2.17	0.8702
Mn-55	6.52	0.0015

The found  $k_{eff}$  is the effective multiplication factor in the beginning of the campaign. The next stage is to calculate  $k_{eff}$  and  $\rho$  throughout the campaign. The result of the calculation of  $k_{eff}$  and  $\rho$  in the beginning of the campaign are given in table 3.

**Table 3.** The result of calculation of keff and reactivity

$\eta$	f	P	$\varepsilon$	$P_{FNL}$	$P_{TNL}$	$k_{eff}$	$\rho$
2.04	0.5984	0.8904	1.02	0.944	0.994	1.040	0.038

## 6. Computation of reactivity change during the campaign

During burnout of the fuel in the reactor, various nuclides are formed in it. Some of them are fissile, while others are poisonous elements. Fissile nuclides include: Pu239, Pu240, and Pu241. As the density of Pu240 is relatively low in comparison to the density of U238, then the fission of Pu240 by fast neutrons is neglected.

Average cross-sections of fission and absorption in the Maxwell spectrum of aforementioned elements:  $\sigma_a^0 = 1588.9$  barns,  $\sigma_f^0 = 940.7$  barns,  $\sigma_a^1 = 169.1$  barns,  $\sigma_f^1 = 1188.5$  barns,  $\sigma_f^2 = 886.5$  barns.

The average neutron flux density:

$$\bar{\Phi} = \frac{3,1 \cdot 10^{10} \cdot N_{th}}{\sigma_f^5 \cdot N_5 \cdot V_{fuel}} \quad (18)$$

Where  $N_{th} = 175$  MWth is the thermal power of the reactor,  $N_5 = 0.213 \cdot 10^{22} \text{ cm}^{-3}$  is the initial density of  $U^{235}$ .  $V_{fuel} = 366606 \text{ cm}^3$  is the volume of the fuel in the core.  $\bar{\Phi} = 2.68 \cdot 10^{13} \text{ n}/(\text{cm}^2 \text{ s})$ .

Effective time:

$$z = \bar{\sigma}_a^5 \bar{\Phi} t \cdot CF, \quad (19)$$

Where  $CF = 0.65$  is the net capacity factor according to the data of JSC OKBM Afrikantov [5].

According to [6] the total thermal energy yield in the reactor campaign is  $4.5 \cdot 10^6 \text{ TW} \cdot \text{h}$ . Therefore, reactor campaign lasts for 1074 effective days (2.93 effective years), which equals 4.52 years taking CF into consideration.

By the formulae given in [7] the densities of all fissile materials are calculated, assuming that density of  $U^{238}$  and the average neutron flux density are constant (Figure 5).

Also, the appearance of different non-fissile nuclides with a large neutron absorption cross-section should be taken into account. These nuclides are classified to poisons, which have a short half-life period, and slags, which are long-lived or stable fission products.

To take into account the increase of reactivity due to the burnout of burnable absorber rods it is necessary to calculate the dependence of gadolinium density on time by following equation:

$$y = N_{Gd}(t) / N_{Gd}(0) \quad (20)$$

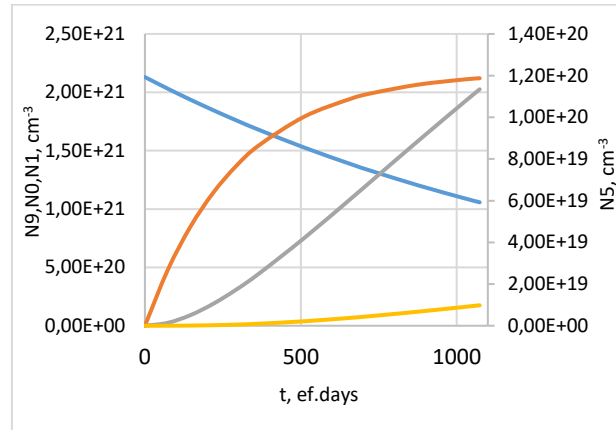


**Figure 5.** The change of densities of fissile nuclides. The blue line is the density of U235, the orange line is the density of Pu239, the grey line is the density of Pu240, and the yellow line is the density of Pu241.

$$x = N_5(t) / N_5(0) \quad (21)$$

Then:

$$y = x^{\sigma_{Gd}/\sigma_5} \exp[\gamma_d \Sigma_{Gd,0}^{ef} (1 - y)] \quad (22)$$

After the dependence of Gadolinium density is known, it is feasible to determine the shielding coefficient throughout the campaign:

$$k_s(t) = \frac{1}{1 + \gamma_d \Sigma_{Gd,0}^{ef} N_{Gd}(t) / N_{Gd}(0)} \quad (23)$$

Having calculated effective multiplication factor using calculated data for core materials it is possible to draw a reactivity change curve, which reveals the change of reactivity during campaign.

The curve in Figure 6, or rather the peak of the curve defines the total weight of control rods that are used to compensate the excessive reactivity. The total weight of the rods should be at least  $\rho_{cr} = 0.209$ .

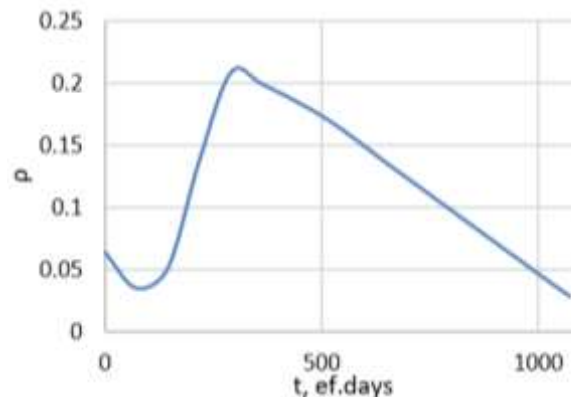


**Figure 6.** Reactivity change curve.

## 7. Conclusion

As it was deduced from the total thermal energy yield, the reactor may operate for 1074 effective days, which concurs with the results of the calculation shown in Figure 6. Also, it can be inferred from Figure 6 that at the end of campaign  $\rho = 0.028$ , which is enough to supply engines of the icebreaker to convey it to the refuelling point.

In addition, Figure 6 reveals that gadolinium burns out too quickly – in the first third of the campaign. The possible reason is the usage of the diffusional approach for calculating the shielding coefficient. Another approach that can be utilized to determine the shielding coefficient is the Wigner approach.

## References

- [1] Deyev V I, Schukin N V, and Cherezov A L 2012 *Principles of Calculation of Nuclear Marine Propulsion* (Moscow: NRNU MEPhI Press) p 256
- [2] Masterson R E 2017 *Nuclear Engineering Fundamentals: a Practical Perspective* (Boca Raton : CRC Press) p 988
- [3] Masterson R E 2017 *An Introduction to Nuclear Reactor Physics* (Boca Raton : CRC Press) p 1107
- [4] Merzlikin G Y 2011 *Nuclear Reactors Theory* (Sevastopol: Sevastopol State University Press) p 341
- [5] *RITM-200 Nuclear Marine Propulsion for New-generation Ice-breakers* (Nizhny Novgorod: JSC OKBM Afrikantov) p 20
- [6] Kudinovich I V 2016 *Nuclear Propulsions of Promising Civil Marine Objects and the Safety Justification* (Saint-Petesburg: The Krylov State Research Centre) p 292
- [7] Dementyev B A 1986 *Nuclear Reactors Control and Kynetics* (Moscow: Energoatomizdat) p 272